American Mineralogist, Volume 91, pages 609–618, 2006

Water in the interlayer region of birnessite: Importance in cation exchange and structural stability

ELIZABETH A. JOHNSON[1,2,*] AND JEFFREY E. POST[1]

[1]Smithsonian Institution, Department of Mineral Sciences, National Museum of Natural History, MRC 0119, Washington, D.C. 20560-0119, U.S.A.
[2]University of California, Los Angeles, Department of Earth and Space Sciences, 595 Charles Young Drive East, 3806 Geology Building, Los Angeles, California 90095-1567, U.S.A.

ABSTRACT

Birnessite is an important scavenger of trace metals in soils and aqueous environments. The basic birnessite-type structure consists of sheets of Mn octahedra separated by ~7 or ~10 Å ("buserite") interlayer regions filled with cations and water. Synthetic birnessite-like structures were produced through cation exchange reactions with synthetic Na-birnessite. The unheated, synthetic Mg^{2+}, Ca^{2+}, and Ni^{2+} layer structures have an ~10 Å interlayer spacing, whereas the other cation-exchanged synthetic birnessites and the related mineral chalcophanite have an interlayer spacing of ~7 Å. The Li^+, Na^+, K^+, Cs^+, and Pb^{2+} synthetic birnessites each contain two to three structurally different water sites, as evidenced by multiple H_2O bending and stretching modes in the infrared spectra. The complexity of the water bands in these spectra is likely related to disordering of cations on the interlayer sites. H-birnessite contains structural water and either hydroxyl, hydronium (H_3O^+), or both. The small difference in the width of the water stretching modes between room temperature and –180 °C indicates that the water molecules in birnessite-like structures are predominantly structurally, rather than dynamically, disordered. Most of the synthetic birnessites, including Na- and K-birnessite, undergo significant water loss at temperatures below 100 °C. There is a linear relationship between the temperature at which most of the water is lost from a given cation-exchanged birnessite and the heat of hydration of the interlayer cation. This finding implies that the interlayer water is strongly bound to the interlayer cations, and plays an important role in the thermal stability of birnessite-like structures.

Keywords: Birnessite, electron microscopy, IR spectroscopy, order-disorder, thermodynamics, XRD data

INTRODUCTION

Birnessite and birnessite-like layer structure minerals, such as chalcophanite and "buserite," are common Mn oxides in soils, stream deposits, and ocean-floor ferromanganese crusts and nodules (Taylor et al. 1964; McKenzie 1976; Burns and Burns 1977; Potter and Rossman 1979a; Post 1999). Birnessite-like layer structures are also used as cathode material in rechargeable Li batteries and are being developed as ion-exchange materials for industrial use (Golden et al. 1986; Bach et al. 1995; Cai et al. 2002). It has been shown that cations are preferentially adsorbed or incorporated into the birnessites in aqueous environments and in soils (McKenzie 1976). Birnessites therefore play an important role in the sequestration and release of nutrients and toxic elements into the environment.

Despite their importance in geochemical cycles, it has been challenging to understand the crystal structure of birnessite and birnessite-like minerals due to the extremely small grain size of natural and synthetic samples, poor crystalline order in many samples, and the strong absorption by Mn of visible and infrared radiation. The chemical formula of birnessite, $Na_{0.7}Ca_{0.3}Mn_7O_{14}{\cdot}2.8H_2O$, was first reported by Jones and Milne (1956). Natural samples were also found to contain trace amounts of a variety of cations, including Co, Ni, and Pb (McKenzie 1977). Various synthetic birnessite-like structures containing almost every alkali and alkali earth element, as well as many of the transition metals, have been produced in the laboratory (e.g., McKenzie 1971; Golden et al. 1986).

Careful analysis of X-ray diffraction (XRD) patterns and infrared spectroscopic data of the structural modes of natural and synthetic birnessites showed that birnessites and "buserite" have a layer structure similar to that of chalcophanite (Giovanoli et al. 1970a, 1970b; Potter and Rossman 1979b). More recently, XRD studies have produced a more detailed understanding of the birnessite and birnessite-like structures. These studies revealed several variations on the birnessite layer structure (e.g., Post and Appleman 1988; Post and Veblen 1990; Kuma et al. 1994; Drits et al. 1997; Lanson et al. 2000).

The basic birnessite structure is triclinic (Post et al. 2002; Drits et al. 2002a) and consists of sheets of Mn^{4+} octahedrally coordinated by O, separated in the ***c***-direction by layers of cations and water molecules arranged in hexagonal close packing (Fig. 1; Post and Veblen 1990). Natural birnessite samples have a ~7 Å interlayer spacing (e.g., Jones and Milne 1956). A natural phase typically found in hydrous environments that is similar to birnessite except for its ~10 Å interlayer spacing is often called by

* E-mail: johnsoel@ucla.edu

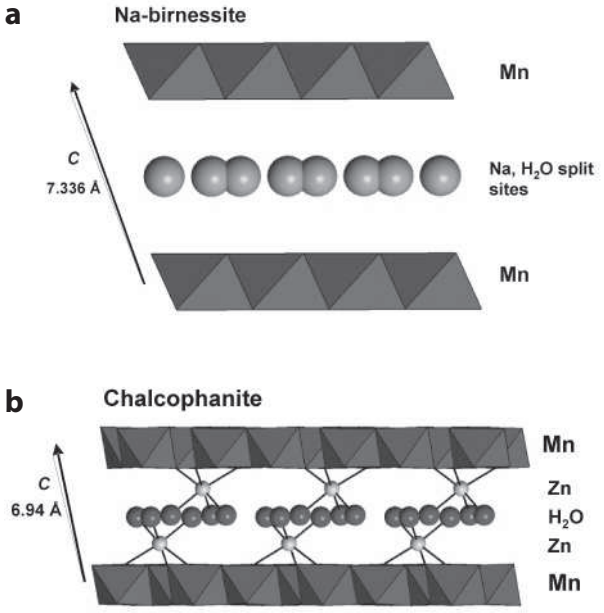

FIGURE 1. Structures of (**a**) synthetic Na-birnessite with disordered interlayer sites containing Na and H_2O (Post and Veblen 1990), and (**b**) chalcophanite (Post and Appleman 1988) containing distinct Zn and H_2O interlayer sites. Plotted using XtalDraw (Downs and Hall-Wallace 2003).

the unapproved name "buserite" (Giovanoli 1980). The samples used in the current work are principally synthetic materials, and the term "birnessite-like" will be used when referring to both the ~7 and ~10 Å phases. Although the changes in interlayer spacing of synthetic birnessite-like structures upon drying from aqueous solution have not been thoroughly investigated, at least some birnessite-like layer structures such as Na-birnessite have a ~10 Å interlayer spacing when synthesized in aqueous solution but form ~7 Å layer structures when dried in air (Wadsley 1950). Other structures like Ca-, Mg-, and Ni-birnessite typically retain the ~10 Å layer spacing upon drying at room temperature (Golden et al. 1986). In Na-, K-, and Cs-birnessite, the interlayer cations and water are disordered over split or diffuse sites elongated in the ***a***-direction within the interlayer plane, and the amount of streaking in electron diffraction patterns increases with increasing cation size (Post and Veblen 1990; Kuma et al. 1994). Electron diffraction studies also have provided evidence for superstructures in the ***a-b*** plane for Li-, Na-, K-, Cs-, Mg-, Ca-, Sr-, Ba-, Ni-, and Pb-birnessites that indicate at least some degree of short-range ordering of cations and water molecules within the interlayer (Post and Veblen 1990; Kuma et al. 1994; Drits et al. 1997, 2002b).

Chalcophanite, $ZnMn_3O_7 \cdot 3H_2O$, has a ~7 Å spacing between layers, and a well-ordered but complex structure in the interlayer region (Fig. 1; Wadsley 1955; Post and Appleman 1988). In chalcophanite, which has trigonal symmetry, one out of every seven Mn^{4+} octahedral layer sites is vacant. There are two layers of Zn^{2+} and one layer of water molecules within the interlayer region. The Zn cations sit above and below the Mn vacancies, and are octahedrally coordinated by three O atoms from the Mn oxide layer structure and three water O atoms within the interlayer. Mg-birnessite, obtained by heating the ~10 Å "Mg-buserite" under vacuum at 105 °C (Golden et al. 1986), has an interlayer region with a structure similar to chalcophanite (Post and Veblen 1990). There must be either some Mn^{3+} or Mn vacancies, or both, within the octahedral layer for charge balance, but there are fewer than in the chalcophanite structure, and these are not necessarily ordered within the layer as in chalcophanite (Post and Veblen 1990; Drits et al. 1997). There is also likely disorder over the water and interlayer Mg cation sites, as three of the water-water distances reported by Post and Veblen (1990) are less than 2 Å and cannot be occupied simultaneously.

Finally, the structure proposed for H-birnessite is hexagonal, has a ~7 Å interlayer spacing, and contains rows of vacancies and Mn^{3+} along [010] within the octahedral sheets of Mn^{4+} (Drits et al. 1997; Lanson et al. 2000). It has been hypothesized that Mn^{2+} and Mn^{3+} sit within the interlayer region, above and below the octahedral layer vacancies, and that hydroxyl groups are attached to layer O atoms adjacent to vacancies and extend into the interlayer region (Lanson et al. 2000).

The XRD studies of birnessite-like phases are generally not able to resolve distinct water and cation sites, but yield positions of water O atoms within the interlayer, or disordered, split sites that are occupied by both interlayer cations and water. Although focused mainly on structural Mn-O modes, Potter and Rossman (1979b) also obtained infrared spectra of the water modes in birnessites and chalcophanite. They concluded that chalcophanite has a single type of structural water defined by a single water bending mode and two stretching modes in the infrared spectrum. The water bands of the natural and synthetic Na- and K-birnessites are broader and more difficult to resolve, but the three modes in the stretching-mode region were interpreted as being caused by one hydroxyl and one water site (Potter and Rossman 1979b).

The purpose of this study is to better understand the structure and bonding environments of water in the interlayer region of synthetic cation-exchanged birnessites and chalcophanite. Variable-temperature infrared spectroscopy has been used to evaluate the type of hydrous species, the number of crystallographic water sites, and the degree of bonding to the interlayer cations for water in each structure, as well as the role water plays in the stability of the birnessite structure upon heating.

METHODS

The starting material for exchange experiments was a synthetic Na-birnessite, made at the Pennsylvania State University by Christina Lopano by adding a solution of 55 g of NaOH in 250 mL H_2O to 200 mL of 0.5 *M* $MnCl_2$ at room temperature, then bubbling oxygen into the mixture for several hours, washing the precipitate with deionized water, and drying the product when needed (Golden et al. 1986, 1987). Table 1 summarizes the experimental conditions for the exchange experiments. The H-, K-, Cs- Ca-, Ni-, and Pb-birnessites were produced by stirring 4–17 mg of the synthetic Na-birnessite in a solution of the appropriate chloride or nitrate salt for 17–72 h. The volume of each solution (50–1400 mL) used was such that the number of exchanging cations in solution was much larger than the amount of Na in the starting birnessite material. Exchange products were filtered and washed with distilled water and dried in air at room temperature. The pH of the H-birnessite exchange solutions was measured at the start and finish of each exchange experiment. The pH of the other exchange solutions was not measured in this study, but the pH of similar cation-exchange solutions was determined to be 5.5 in a previous study (Golden et al. 1986). The Li-birnessite and Mg-buserite were created by exchange of about 2 mg of Na-birnessite with 40 mL of 1 *M* solu-

TABLE 1. Experimental conditions and results for cation exchange between synthetic Na birnessite and aqueous solutions at room temperature

Cation exchanged	Exchange solution	Exchange time (hours)	EDS Remaining Na?	EDS Exchanged cation present?	Interlayer spacing *d* (001) (Å)	Structural IR modes (cm^{-1})	Water bending mode (cm^{-1}) §	T of 85% dehydration (°C)
H pH=2	0.01 M HCl	21	no	na	7.26	746, 660, 577, 503, 455, 380	1630	182
H pH=3	0.001 M HCl	19	no	na	7.24			
H pH=3.8	0.00016 M HCl	23	no	na	7.27			
Li*	1 M LiCl	120	yes	na	6.96	723, 644, 515, 482, 426, 372	1635	130
Na*	na	na	na	na	7.24	638, 515, 480, 420, 363	1628	126
K	1 M KCl	22	no	yes	7.08	637, 515, 482, 419, 376	1622	129
Cs	0.5 M $CsNO_3$	72	no	yes	7.37	633, 515, 490, 447, 424	1614	109
Mg†	1 N $MgCl_2$	17	no	yes	6.96	702, 633, 517, 480, 430, 384, 355	1641	246
Mg-buserite*	1 M $MgCl_2$	120	no	yes	9.49, 7.04	638, 517, 484, 426		268
Ca	1 M $CaCl_2$	23.5	no	yes	9.96, 7.31	640, 519, 492, 426	1620	202
Ni	1 M $NiCl_2$	48	no	yes	9.63	760, 642, 513, 482, 422, 368	1603	205
Chalcophanite (Zn)‡	na	na	na	na	6.92	802, 667, 625, 594, 532, 498, 474, 438	1630	278
Pb	0.5 M $Pb(NO_3)_2$	18	yes	yes	7.11	640, 513, 482, 422, 368	1640	153

Note: na= not applicable to this sample.
* Made at PSU
† Sample from Golden et al. 1986. After exchange, sample was dried at 105°C under vacuum.
‡ Chalcophanite sample NMNHC1813 from Leadville, CO.
§ Obtained from spectra of thin films at room temperature.

tion of chloride salt. The exchange product was centrifuged and 40 mL of new solution was added each day for five days, for a total of 200 mL of solution used for each exchange (syntheses done by Christina Lopano at the Pennsylavania State University). The Mg-birnessite was provided by D.C. Golden, and was produced by dehydrating Mg-buserite, produced as described above, under vacuum at 105 °C (Golden et al. 1986). The chalcophanite sample NMNH no. C1813 is from Leadville, Colorado.

For XRD studies, the exchange products were sieved to 325 mesh to break up clumps of dried material, and loaded into 0.5 mm quartz glass capillaries. X-ray powder patterns were obtained on a Rigaku DMax Rapid X-ray diffractometer fitted with an imaging plate, using a 0.3 mm collimator with Mo$K\alpha$ radiation. Capillaries were rotated at 1 degree per second on phi, and total count time was 10 min for each sample.

The exchange products were analyzed with energy-dispersive spectroscopy (EDS) using a JEOL JSM-840A scanning electron microscope, 15 kV accelerating voltage and a 0.47 nA beam current. Back-scattered electron (BSE) images were obtained for each exchange product to confirm sample homogeneity.

Infrared spectra were obtained at room temperature and at –180 °C using KBr pellets, and from room temperature to as high as 350 °C with thin films of the birnessite-type exchange products. For the KBr pellets, approximately 1 mg of Mn oxide and 250 mg of KBr were ground in a mill for at least 1 min, and pressed under vacuum for 2 min. The thin films were created by making slurries of the Mn oxide in water or ethanol that were deposited on a BaF_2 window and dried at room temperature (21 °C) in air.

Spectra were collected using a Digilab Excalibur FTS3000 spectrometer with a KBr beamsplitter at 4 cm^{-1} resolution, and were averaged over 256 scans. In the main compartment, transmission spectra were obtained at room temperature on the KBr pellets over the range 350–6000 cm^{-1} using a DTGS detector.

In situ low- and high-temperature studies were carried out using a Linkham Scientific Instruments FTIR600 heating and cooling stage with ZnSe windows on a UMA-500 microscope with an MCT detector. The cooling and heating rate was 10 °C per min. Temperature was monitored with a platinum resistor sensor, and was shown to be accurate to ±0.1 °C through calibration with various melting points and solid-state transitions.

The percent loss of water at a given temperature during the in situ heating was determined by integrating the total band area in the OH-stretching region (3000–3600 cm^{-1}) using a linear background and ratioing to the room temperature value. Integration of OH band areas is a technique regularly used for quantification of hydrous species in nominally anhydrous minerals (e.g., Johnson and Rossman 2003), and unlike band intensity measurements, band areas are not affected by changes in peak shape during heating or cooling. This method assumes that the infrared absorption coefficient does not vary significantly over the limited energy range of OH-stretching modes for the different water species found in each birnessite (Paterson 1982; Libowitzky and Rossman 1997).

RESULTS AND DISCUSSION

EDS data

The EDS analyses of the birnessite-like phases resulting from the exchange experiments are listed in Table 1. For all of the experiments except the Li and Pb exchanges, no detectable Na remained in the birnessite, and the exchanged cations detectable by EDS were confirmed to be present in the birnessite. In all cases, the exchange solutions contained excesses of the cation to be exchanged, so (apparently) at room-temperature conditions and near-neutral pH, Li and Pb do not completely exchange for Na in the birnessite interlayer. Although Golden et al. (1986) reported a successful exchange of Li for Na in synthetic birnessite, they did not evaluate the composition of the exchange product. The EDS results for the current study show that approximately 20% of the initial Na concentrations remain in the Li- and Pb-exchanged birnessites. All of the exchanges produced homogeneous products that were often finer-grained than but otherwise resembled the platy morphology of the starting synthetic Na-birnessite in BSE and secondary electron (SE) images.

X-ray diffraction

The XRD patterns confirm that the exchange products are birnessite-type structures, and they reveal two general categories of layer structure: one with ~7 Å layer spacing and the other with ~10 Å layer spacing (Fig. 2). Table 1 lists the interlayer spacing for each exchange product calculated from 2θ values of the (001) peaks, using a value of 0.71069 Å for the wavelength of the Mo$K\alpha$ radiation. Of the birnessite-like structures in this study, only the Ca-, Mg-, and Ni-birnessites have a predominantly ~10 Å interlayer spacing in air. These birnessite-like structures have either been partially (less than 10%) dehydrated, or the layer structure was not completely expanded during exchange, as evidenced by the presence of a minor ~7 Å peak in the Ca-, Mg-, and Ni-birnessite diffraction patterns. Chalcophanite and the Pb-exchanged birnessite have a ~7 Å interlayer spacing,

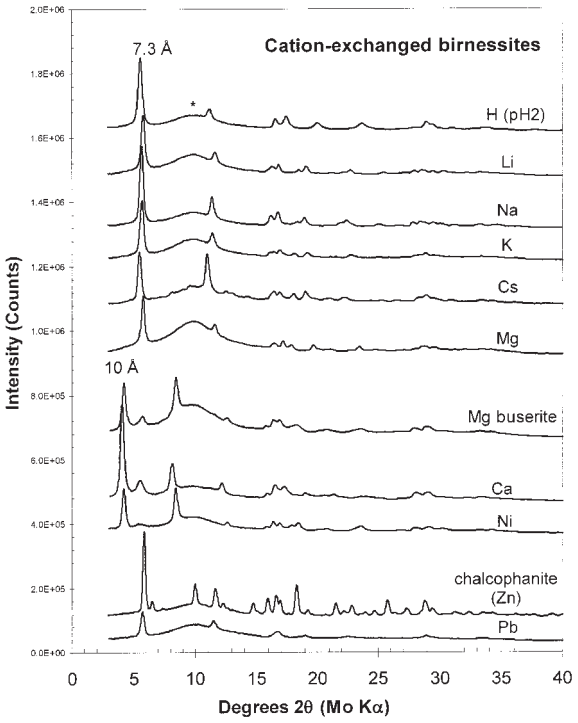

FIGURE 2. Powder XRD patterns (Mo$K\alpha$ radiation) of cation-exchanged birnessites. The (001) peaks corresponding to the interlayer distances (~10 and ~7 Å) are labeled. The asterisk (*) marks the position of the broad peak due to the glass capillary.

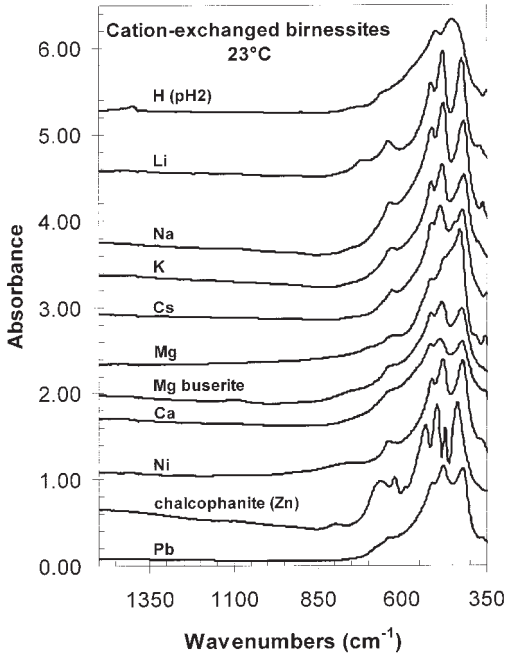

FIGURE 3. Mid-IR spectra (350–1450 cm^{-1}) of the structural Mn-O modes of the cation-exchanged birnessites, obtained from KBr pellets at room temperature.

even with the presence of divalent interlayer cations. No specific relationship between ionic radius and birnessite interlayer spacing was found (Table 1).

IR spectra of structural modes

The mid-infrared transmission spectra in the 350 to 1400 cm^{-1} region, taken on KBr pellets at room temperature, are shown in Figure 3. The general positions of the Mn-O bands are the same as those reported for natural and synthetic birnessites and todorokite by Potter and Rossman (1979b), although the band widths are in general narrower for the synthetic samples than for the natural samples. Most of the exchanged birnessites have nearly identical spectra in this region. The relative band intensities of the Mg-birnessite spectrum are different from other synthetic birnessites, but this minor difference is attributed to the fact that this Mg-birnessite sample, donated by D.C. Golden, underwent heating under vacuum as part of the synthesis process (Golden et al. 1986). The H-birnessite and chalcophanite spectra are significantly different from the others. The H-birnessite has broader bands centered near 460 and 494 cm^{-1} rather than at 422, 482, and 515 cm^{-1}. The natural chalcophanite has additional bands at 474 and 600–802 cm^{-1}.

There is no correlation between the frequency of the various bands in the 350–800 cm^{-1} region and the size or charge of the interlayer cation. This is an expected result as absorbance in this region is primarily due to the vibrational modes of the Mn octahedra within the octahedral layer. Potter and Rossman (1979b) noted that broadening of structural modes in the infrared spectra is not related to disorder measured by XRD. Unlike XRD, infrared spectroscopy does not detect long-range order or disorder in the crystal structure. Instead, infrared spectroscopy is more sensitive to grain size and local differences in bonding environments. These local differences for the octahedral layer include a range in the number of shared edges of the Mn octahedra (Potter and Rossman 1979b) due to vacancies in the Mn octahedral layer sites or local disordering of the structure, and may also reflect variations in Mn-O distances due to the presence of Mn^{3+} or Mn^{2+} in the octahedral layer structure or interlayer region (Post and Veblen 1990). The greater range of oxidation state of the Mn proposed by Drits et al. (1997) and Lanson et al. (2000) in the H-birnessite interlayer region, compared with that of the other synthetic birnessites, could significantly contribute to the broadened absorption features in this region for the H-birnessite. The ordered vacancies in the Mn oxide layers of chalcophanite result in Mn octahedra with only five shared edges instead of six, and could be responsible for the additional modes observed in the infrared spectrum of chalcophanite.

IR spectra of hydrous species

The water stretch and bend modes for all of the birnessites are found at 3000–3600 and ~1600 cm^{-1}, respectively, and are within typical energy ranges for water molecules bound in a mineral structure (Lutz 1988) (Fig. 4). Spectra were also obtained at –180 °C to better resolve individual bands by reducing the broadening effect due to any librational or rotational motion of the water molecules. The OH-stretching modes of the monovalent cation-exchanged birnessites sharpened slightly between 23

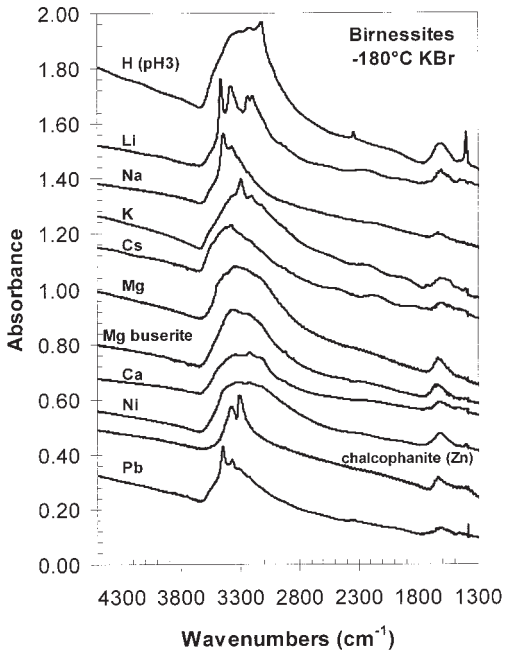

FIGURE 4. Mid-IR spectra (1300–4500 cm^{-1}) of the hydrous species in the interlayer of synthetic birnessites, obtained at –180 °C from KBr pellets. Water-bending modes are found near 1600 cm^{-1}, and water-stretching modes are between 3000–3500 cm^{-1}. Sharp bands at 1300 and 2300 cm^{-1} in the H-birnessite spectrum are due to hydroxyl or hydronium, H_3O^+.

and –180 °C, which is an indication that there is some dynamic disordering of water at room temperature. Other than the Mg-birnessite and Mg-buserite discussed above, the birnessite-like phases substituted with divalent cations in the interlayer with ~10 Å layer spacings have broader and more poorly resolved OH stretch modes than those with ~7 Å layer spacings like Pb-birnessite, and those with monovalent cation substitutions. This difference implies that there is greater positional disorder for water over the greater number of sites in the expanded interlayer region of the divalent cation-exchanged birnessites.

In detail, each cation-exchanged birnessite has a different spectrum in the 3000–3600 cm^{-1} region. In most solid hydrates, each type of structural water molecule produces a pair of symmetric (υ_1) and antisymmetric (υ_3) stretching vibrational modes (Lutz 1988). The difference in energy between υ_1 and υ_3 can be as little as 80 cm^{-1} or up to more than 200 cm^{-1} (Lutz 1988). The average energy of the υ_1 and υ_3 modes is similar for all of the birnessite exchange products, implying that the degree of hydrogen bonding between the water and the O atoms within the Mn layers of the birnessite is similar for all of the samples (Nakamoto et al. 1955; Libowitzky 1999). Using the empirical relationship between hydrogen bonding distance and infrared frequency of the stretching modes of hydrous species (Libowitzky 1999), the average O-H···O distance in the birnessite-like structures is about 2.74 Å, with a possible total range of distances between 2.67 and 2.89 Å. This range is similar in value to the distances between water-oxygen atoms (O2) within the interlayer and O atoms in the Mn-O octahedral layer determined from X-ray structure refinements for Na-, K-, and Mg-birnessites (2.57–3.02 Å, Post and Veblen 1990), Na-binessite (2.69–2.71 Å, Lanson et al. 2002a), and Pb-birnessite (2.66 Å, Lanson et al. 2002b). There could also be one or more distinct hydroxyl groups in the birnessites with multiple narrow bands in the OH-stretching region, but it is not possible to distinguish modes due to hydroxyl from bands due to water molecules using this region of the spectrum alone because of multiple overlapping bands.

All of the spectra in Figure 4 have at least one bending mode of water at around 1600 cm^{-1}, indicating the presence of one or more types of H_2O in the structure. In some cases, such as the Li-birnessite, two water bending modes and four major stretching modes indicate the presence of two different types of structural water. The average energy of the water bending mode decreases with increasing ionic radius of the interlayer cation (Fig. 5). Pb-birnessite falls off of the trend in Figure 5. An increase in the range and absolute values of Pb-O distances in Pb-bearing minerals such as hyalotekite has been observed and is attributed to the Pb^{2+} $6s^2$ lone-pair effect (Moore et al. 1982, 1985). A correction for the lone-pair effect would increase the effective ionic radius of Pb^{2+} in the birnessite structure, shifting Pb-birnessite to the right on Figure 5 and bringing it into closer alignment with the other data.

Previous studies have found that increasing the strength of hydrogen bonding of structural water and decreasing the H-O-H intramolecular angle both act to increase the energy of the water bending mode in solid hydrates, although increased metal to water- oxygen bonding has the opposite effect on the energy of the water bending mode (Lutz 1988). In this study, however, an increasing trend is not observed in the energy of the water bending mode as a function of hydration energy (ΔH), a measure of water-cation bond strength (see below). Therefore, metal to water-oxygen bonding interactions in the birnessite interlayer region do not have a major effect on the water bending-mode energy. It is also not likely that differences in the strength of hydrogen bonding of water in the interlayer region are the predominant cause of the trend in Figure 5 because, as was pointed out above, the average water stretching mode and thus the average water-oxygen to structural-oxygen distance is almost identical for all of the cation-exchanged birnessites (Libowitzky 1999). The remaining possibility is that synthetic birnessites containing larger cations such as Cs^+ and Ca^{2+} have interlayer water molecules with larger H-O-H intramolecular angles than those in birnessites with smaller interlayer cations such as Li^+ and Mg^{2+}. The water molecules in Cs-birnessite might have more distorted geometries than those in Li-birnessite to coordinate to the larger Cs^+ ion within the plane of the interlayer. The H-birnessite spectrum has additional bands at 1300 and 2300 cm^{-1} that sharpen significantly upon cooling to –180 °C. These bands may be assigned either as vibrational modes of hydronium, H_3O^+, or as a librational mode of hydroxyl and a combination rotational-bend mode for water, respectively (Wilkins et al. 1974).

The stretching plus bending combination modes of the hydrous species are not observed or are poorly resolved for most of the exchanged birnessites, due to the strong Mn^{3+}-Mn^{4+} intervalence charge transfer absorbance band that extends into the near-infrared region. The Na-, Ca-, and Pb-birnessites and chalcophanite have broad bands (100–400 cm^{-1} FWHM) centered between 4800 and 5200 cm^{-1} that are within the accepted

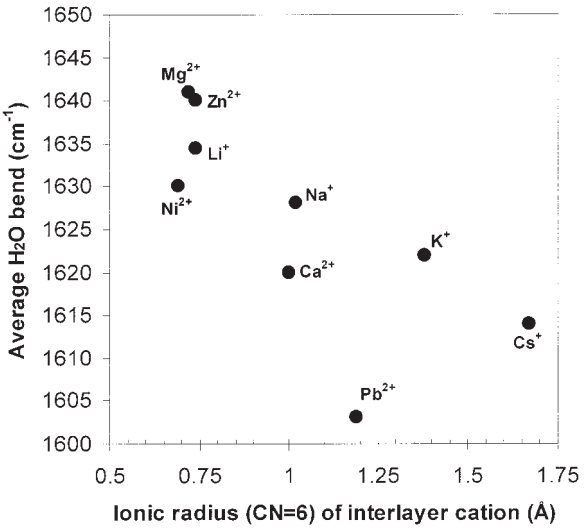

FIGURE 5. The average energy of the water bending mode vs. the ionic radius of the interlayer cation, in sixfold coordination. Ionic radii are from Shannon (1976).

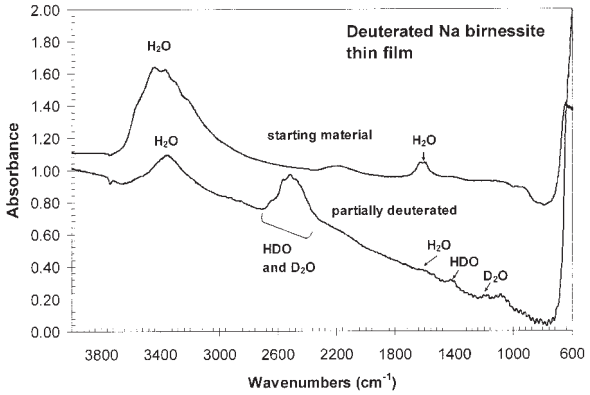

FIGURE 6. Infrared spectra of the hydrous species in H_2O-bearing and partially deuterated Na-birnessite. The vibrational modes of H_2O are at 1632, 3550, and 3371 cm^{-1}; HDO modes are at 1429 cm^{-1} and between 2700 and 2300 cm^{-1}, and D_2O modes at 1199 cm^{-1} and between 2700 and 2300 cm^{-1}.

energy range for symmetric stretch plus bend combination modes for crystallographically bound molecular water (Appendix 1; Stolper 1982; Johnson and Rossman 2003). The H-birnessite has an additional combination mode at about 4640 cm^{-1}, which could be assigned to a stretch plus bend combination mode of hydronium (Wilkins et al. 1974), or a stretch plus librational combination mode of hydroxyl (Stolper 1982). Proton mobility in the interlayer could produce both hydroxyl and hydronium through the reaction, $2H_2O = OH^- + H_3O^+$ (Wilkins et al. 1974). The spectroscopic data confirms that there is another hydrous species in addition to H_2O molecules present in H-birnessite, but cannot differentiate between hydroxyl (Drits et al. 1997), hydronium, or both, as the additional interlayer species.

Partially deuterated Na-birnessite was obtained by stirring about 10 mg of the Na-birnessite starting material in 25 mL D_2O for 12 h, then directly depositing a slurry of the birnessite in D_2O onto a BaF_2 window that was immediately enclosed in the heating and cooling stage under dried air at room temperature. A spectrum was produced with absorption due to the vibrational modes of H_2O (1632, 3550, and 3371 cm^{-1}), HDO (1429 cm^{-1} and modes between 2700 and 2300 cm^{-1}), and D_2O (1199 cm^{-1} and modes between 2700 and 2300 cm^{-1}) (Fig. 6). This result confirms that the bands from 1600–3500 cm^{-1} are due to water molecules in the birnessite, and that there are multiple bonding environments for structural water. Assuming that the deuteration process did not go to completion during the exchange process, the water sites responsible for the narrow, complex OH-stretching modes were more easily exchanged isotopically than the water site or sites responsible for the broad absorption features in that region that are likely to be more strongly bound within the interlayer. This result is consistent with data from the dehydration experiments discussed below and suggests that the broad modes result from water that is more strongly bound to cations in the interlayer, layer structure O atoms, or both, which would be expected to exchange less rapidly than free interlayer water.

The major features of the mid-IR spectra (1300–4400 cm^{-1}) obtained from the KBr pellets and thin films were nearly identical to each other for each of the cation-exchanged birnessite-like phases (Figs. 7a and 7b). However, the detailed structure of the OH-stretching modes varied according to the method of sample preparation for the H- and Ca-birnessites (Fig. 7c). This difference could be due to reaction of the surface of the birnessite grains with the KBr, or the preferred orientation of the mineral grains in the thin films of these samples, or because the spectra on KBr pellets and thin films were obtained several months apart. In the spectra from thin films of the Na-, Pb-, and Ni-birnessites and the Mg-buserite, the H_2O bend plus rotational mode at 2300 cm^{-1} is present (Wilkins et al. 1974), but is not observed in spectra from the KBr pellets. The spectrum of the Li-birnessite thin film has an additional mode at 1740 cm^{-1} (not present in the spectrum from the KBr pellet of the same sample), which is at the expected frequency of the ν_4 mode of hydronium, H_3O^+ (Wilkins et al. 1974), or could be due to a surface effect.

Heating experiments

Selected results of in situ heating experiments obtained on the IR microscope are shown in Figure 8. Water loss causes a decrease in intensity of all of the water stretching modes for each sample. For almost all of the birnessites, the sharper bands decrease in intensity fairly rapidly, leaving much broader bands that persist to higher temperatures (Figs. 8a and 8b). This is not the case for the spectra of Li-birnessite (Fig. 8c), in which loss of intensity progresses equally for all bands. The birnessites with monovalent interlayer cations dehydrate at lower temperatures than birnessites with divalent interlayer cations. In many samples, especially the Cs- and Pb-birnessites, there is a significant (~25%) loss of water at temperatures as low as 50 °C (Appendix 2), suggesting that it is important to consider possible structural changes upon drying and heating for samples originating in cool, wet environments that contain birnessite-structure minerals.

Spectra were obtained at room temperature at the end of the heating runs on most of the samples, after allowing them to cool to room temperature on the heating stage for 30 min to 2

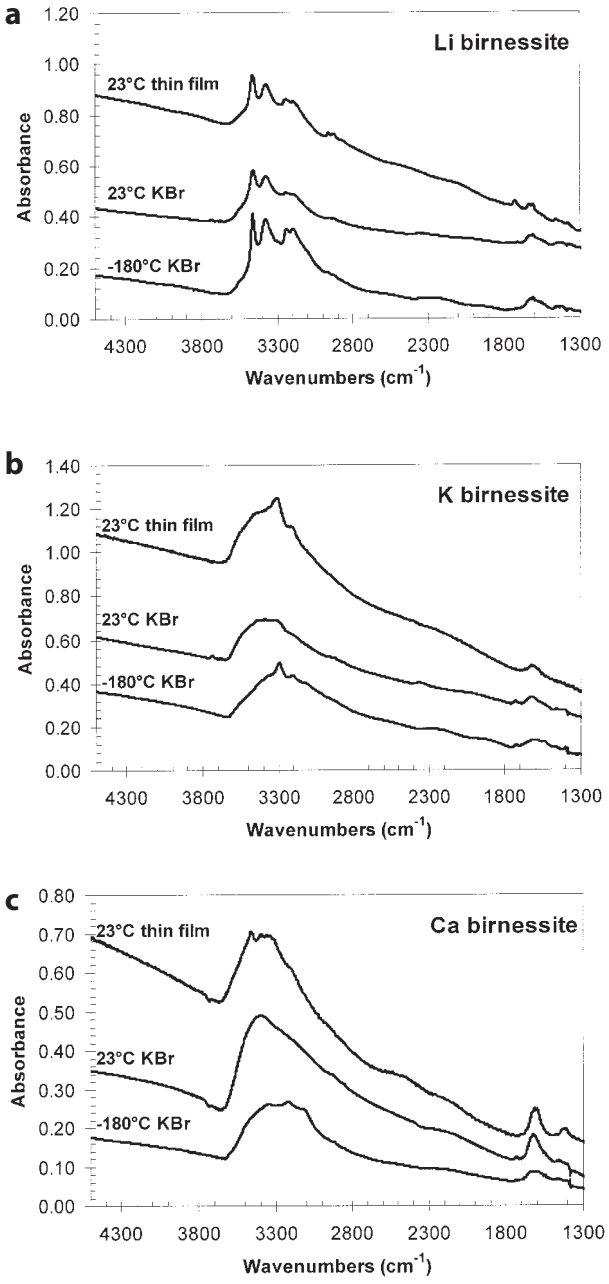

FIGURE 7. Mid-IR spectra obtained on KBr pellets at 23 and –180 °C and thin films at 23 °C for (**a**) Li-birnessite, (**b**) K-birnessite, and (**c**) Ca-birnessite.

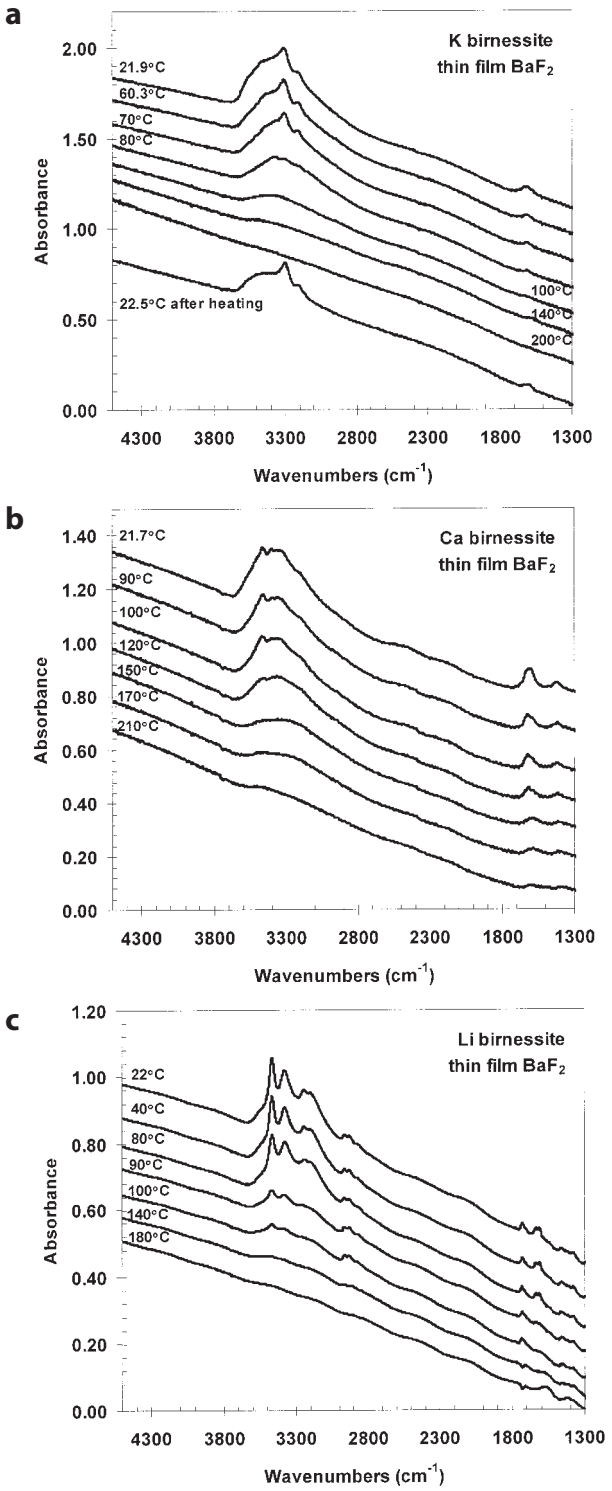

FIGURE 8. Selected infrared spectra of the water region for in situ heating experiments on thin films of (**a**) K-birnessite, (**b**) Ca-birnessite, and (**c**) Li-birnessite.

h under the "dry" air purge. The K-birnessite (Fig. 8a) showed the most dramatic rehydration capacity. After about an hour, the sample regained about half of the original band area of the water-stretching modes, after being heated to a maximum temperature of 140 °C. Other cation-exchanged birnessites also underwent significant amounts of rehydration after being fully (or almost fully) dehydrated during heating. The Ca-, Mg-, and Ni-birnessites recovered 28, 17, and 13% of their original water contents, respectively. On the other hand, the Li-birnessite only recovered 1% of the initial water concentration, and the Mg-buserite and chalcophanite each rehydrated to 8% of their

previous water content. Apparently the specific interlayer cation within each structure influences its general thermal stability as well as its ability to rehydrate after being heated to a given temperature. Golden et al. (1986) noted that whereas K-birnessite retains its layer structure until 400–600 °C, when it converts to a cryptomelane-type structure, other cation-exchanged birnessites become disordered and change structure at lower temperatures (as low as 200 °C in the case of Li-birnessite).

The temperature at which most (85%) of the water is lost from each sample was determined from the in situ heating measurements (Table 1). This dehydration temperature is plotted in Figure 9 vs. the hydration energy, ΔH, for the different interlayer cation species (Benjamin and Gold 1954; Ball and Norbury 1974). The hydration energy is the enthalpy change involved in solvating a gaseous ion in liquid water at 298 K and 1 atm pressure (Benjamin and Gold 1954; Ball and Norbury 1974). It is effectively a measure of the energy needed to remove the hydration sphere of water from an ion in solution. There is a clear correlation between the temperature of 85% water loss from the birnessite structures and the hydration energy, ΔH (Fig. 9). By influencing the Pb-O geometry and bond distances (Moore et al. 1982, 1985), the Pb^{2+} lone-pair effect could interfere with the analogy between a Pb-H_2O hydration complex in solution and the interlayer structure of Pb-birnessite, and may explain the anomalous position of the Pb-birnessite datum in Figure 9. The temperature reported in Figure 9 might also be somewhat lower (~5 °C) than the true value for the Pb-birnessite, as this sample was not fully exchanged from the Na-birnessite starting material, and the temperature of dehydration for the Pb-birnessite is 25 °C higher than that for Na-birnessite. This data suggests that the water in birnessite is bound to the interlayer cations to a similar degree as inner-sphere water is bound to these cations in an aqueous solution. Birnessite-like structures with larger and lower-valence interlayer cations will dehydrate more rapidly during heating than those with small, higher-valence interlayer cations.

Interlayer water and the birnessite structure

The spectroscopic data (Figs. 4–8) show that all of the cation-exchanged birnessites contain structural water molecules. The

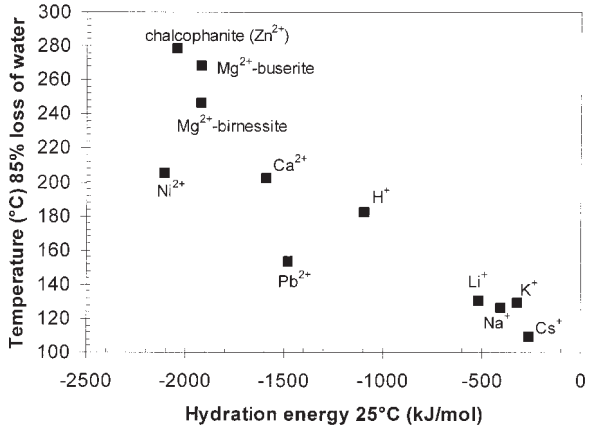

FIGURE 9. Temperature of 85% loss of water from the birnessite structure vs. the hydration energy, ΔH (Benjamin and Gold 1954; Ball and Norbury 1974), of the interlayer cation at 25 °C.

monovalent interlayer cation birnessites and Pb-birnessite that have ~7 Å interlayer spacing have a greater number of distinct and slightly dynamically disordered water sites than those ~10 Å phases containing divalent cations, although both types contain positionally disordered water. The water most strongly bound within the interlayer also has the greatest structural disorder. The natural chalcophanite has strong short-range ordering of layer vacancies, Zn^{2+}, and interlayer water. The H-birnessite contains hydronium or hydroxyl as well as structural water.

The complexity of the water bands for the birnessite-like structures can be explained by combining results from X-ray refinements and infrared spectroscopy. Structural refinements from XRD data located split or diffuse sites in the interlayer that are partially occupied by cations such as Na or K, and water molecules (e.g., Post and Veblen 1990; Kuma et al. 1994). This site splitting increases the number of structurally distinct sites for water molecules. One unique water-bonding environment, with the average OH-stretching modes at about 3200–3220 cm^{-1} (Libowitzky 1999), would be expected from the symmetrically equivalent H_2O split sites in the Na-birnessite model of Lanson et al. (2002a). The Lanson et al. (2002a) model assumes that the two H atoms in each interlayer water are hydrogen bonded to O atoms in the Mn octahedral layer that are 2.69 and 2.71 Å away, respectively. These stretching-mode energies are at the low energy end of the observed OH absorption range for the birnessite-like structures (2900–3600 cm^{-1}; Fig. 3). Although the Lanson et al. (2002a) model describes an important end-member case where interlayer water is hydrogen bonded to O atoms in the layer structure with its H-H vector aligned parallel to the ***c***-axis, it does not explain the multiple hydrogen bonding sites observed at higher vibrational energies (Fig. 3).

The distances between water molecules on the split water sites in the interlayer (2.850, 2.954, and 3.015 Å; Post and Veblen 1990) are longer than the water-oxygen to layer-oxygen distances. An H_2O-H_2O distance of 2.146 Å is also possible according to the model but seems highly unlikely due to the unrealistically strong hydrogen bonding implied by this short distance (Libowitzky 1999). Figure 10 shows one possible scenario for interlayer ordering of H_2O and Na in the synthetic Na-birnessite interlayer, which is similar to the ordering in the NaBi II model of Lanson et al. (2002a), and assumes that the interlayer is perfectly stoichiometric (three water molecules for every Na; Post and Veblen 1990). In this simplified model, every Na atom sits in the center of the split site but H_2O molecules can be positioned at either end of a diffuse site. Two unique but similar interlayer water environments are produced with this model. Interlayer water molecules on these sites with H-H vectors roughly perpendicular to the ***c***-axis would have ν_1 and ν_3 modes between about 3460 and 3555 cm^{-1} (Libowitzky 1999). A birnessite-like structure containing interlayer water sites with H-H vectors both perpendicular to and parallel to ***c***, would therefore have ν_1 and ν_3 H_2O modes between 3200–3220 cm^{-1} and 3460–3555 cm^{-1}, which roughly brackets the range of observed values (2900–3600 cm^{-1}). A third possible interlayer water H-H vector orientation is at an angle to ***c***, with one water hydrogen bonded to an interlayer water-oxygen (2.850–3.015 Å) and the other bonded to an O atom in the Mn layer (2.69–2.71 Å). This orientation predicts a range of water stretch modes with energies

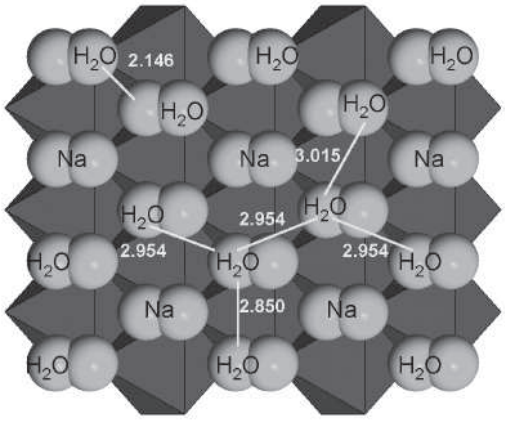

FIGURE 10. One possible model for ordering of Na and H_2O in the interlayer region of synthetic Na-birnessite, projected along the ***c***-axis. Manganese in the layer structure are represented by dark-gray octahedra, and diffuse or "split" interlayer sites are shown in light gray. Distances are in angstroms. The structure is from Post and Veblen (1990); the general interlayer ordering is similar to the NaBi II model of Lanson et al. (2002a). Plotted using XtalDraw (Downs and Hall-Wallace 2003).

intermediate to the two end-member scenarios above. Variable positioning of Na along the diffuse sites, a lack of stoichiometry, disorder within the interlayer, and defects along ordered domains within the interlayer could produce an even greater variety of bonding environments for water in the interlayer of Na-birnessite, and by analogy, the other birnessite-like structures.

In the ~10 Å birnessite structures, water molecules within hydration complexes are bound to the interlayer cations, although these complexes likely occur in a large number of different orientations within the birnessite interlayer. This disordering of H_2O bonding environments, in addition to the greater number of H_2O molecules present in the interlayer region of an ~10 Å birnessite-like structure compared to an ~7 Å phase, explains why the H_2O infrared stretch modes for the ~10 Å structures appear as a single broad absorption feature instead of the sharper bands found in the infrared spectra of the ~7 Å birnessites. However, the presence of complex bonding environments of hydration complexes does not preclude short-range superstructure ordering of cations within the interlayer.

It has been postulated that interlayer water is a major factor in the stability of the birnessite structure when dried in air at room temperature or when heated (Golden et al. 1986; Kuma et al. 1994; Post et al. 2004). The present study confirms this hypothesis by direct observation of the hydrous species with infrared spectroscopy. The hydration energy of the interlayer cation, related to its size and charge, controls the bonding strength between it and the water, which is directly related to the temperature of dehydration and the temperature of collapse of the birnessite structure. In general, the strength of the bonding between the water and interlayer cations determines whether the interlayer distance remains ~10 Å upon drying, or collapses to an ~7 Å structure. For example, Ca-birnessite, with an hydration energy of –1592.62 kJ/mol is an ~10 Å structure when dried, whereas Na-birnessite with a ΔH of –405.49 kJ/mol is an ~7 Å structure after drying (Shannon 1976; Figs. 2 and 9).

Future work involving ab initio modeling of minimum energy configurations of water molecules and cations in the interlayer region is under way and hopefully will better resolve the differences observed in the infrared spectra of birnessite-like structures. A better understanding of the role of water in the stability of the birnessite structure could come from modeling the changes in a particular structure as a function of temperature using a combination of X-ray refinements and infrared spectroscopic data. Eventually, competitive exchange experiments of cations into the birnessite structure (Golden et al. 1986) in conjunction with X-ray and electron diffraction and infrared spectroscopy could aid in our understanding of the structure of the interlayer region in natural samples during exchange with the surrounding environment.

ACKNOWLEDGMENTS

The authors thank P. Heaney, C. Lopano, and G.C. Golden for contributing synthetic birnessites used in this study. This study was funded by NSF grants EAR-0417714 and EAR-0125908 and a postdoctoral grant from the Smithsonian Institution Fellowship program.

REFERENCES CITED

Bach, S., Pereira-Ramos, J.P., and Baffier, N. (1995) Synthesis and characterization of lamellar MnO_2 obtained from thermal decomposition of $NaMnO_4$ for rechargeable lithium cells. Journal of Solid State Chemistry, 120, 70–73.

Ball, M.C. and Norbury, A.H. (1974) Hydration energies. In Physical Data for Inorganic Chemists, p. 52–57. Longman, London.

Benjamin, L. and Gold, V. (1954) A table of thermodynamic functions of ionic hydration. Transactions of the Faraday Society, 50, 797–799.

Burns, R.G. and Burns, V.M. (1977) Mineralogy. In G.P. Glasby, Ed., Marine Manganese Deposits, p. 185–248. Elsevier, Amsterdam.

Cai, J., Liu, J., and Suib, S.L. (2002) Preparative parameters and framework dopant effects in the synthesis of layer-structure birnessite by air oxidation. Chemistry of Materials, 14, 2071–2077.

Downs, R.T. and Hall-Wallace, M. (2003) The American Mineralogist crystal structure database. American Mineralogist, 88, 247–250.

Drits, V.A., Silvester, E., Gorshkov, A.I., and Manceau, A. (1997) Structure of synthetic monoclinic Na-rich birnessite and hexagonal birnessite: I. Results from X-ray diffraction and selected-area electron diffraction. American Mineralogist, 82, 946–961.

Drits, V.A., Lanson, B., Bougerol-Chaillout, C., Gorshkov, A.I., and Manceau, A. (2002a) Crystal structure determination of synthetic Na-rich birnessite: evidence for a triclinic one-layer cell. American Mineralogist, 87, 1662–1671.

——— (2002b) Structure of heavy-metal sorbed birnessite: Part 2. Results from electron diffraction. American Mineralogist, 87, 1646–1661.

Giovanoli, R. (1980) On natural and synthetic manganese nodules. In I.M. Varentsov and G. Grasselly, Eds., Proceedings of the 2nd International Symposium on Geology and Geochemistry of Manganese, 1, p. 159–202. Schweizerbart, Stuttgart.

Giovanoli, R., Stähli, E., and Feitknecht, W. (1970a) Über Oxidhydroxide des vierwertigen Mangans mit Schichtengitter 1. mitteilung: Natrium-Mangan(II,III) Manganat(IV). Helvetica Chimica Acta, 53, 209–220.

——— (1970b) Über Oxidhydroxide des vierwertigen Mangans mit Schichtengitter 2. mitteilung: Mangan(III) Manganat(IV). Helvetica Chimica Acta, 53, 453–464.

Golden, D.C., Dixon, J.B., and Chen, C.C. (1986) Ion exchange, thermal transformations, and oxidizing properties of birnessite. Clays and Clay Minerals, 34, 511–520.

Golden, D.C., Chen, C.C., and Dixon, J.B. (1987) Transformation of birnessite to buserite, todorokite, and manganite under mild hydrothermal treatment. Clays and Clay Minerals, 35, 271–280.

Johnson, E.A. and Rossman, G.R. (2003) The concentration and speciation of hydrogen in feldspars using FTIR and ^{1}H MAS NMR spectroscopy. American Mineralogist, 88, 901–911.

Jones, L.H.P. and Milne, A.A. (1956) Birnessite, a new manganese oxide mineral from Aberdeenshire, Scotland. Mineralogical Magazine, 31(235), 283–288.

Kuma, K., Usui, A., Paplawsky, W., Gedulin, B., and Arrhenius, G. (1994) Crystal structures of synthetic 7 Å and 10 Å manganates substituted by mono- and divalent cations. Mineralogical Magazine, 58, 425–447.

Lanson, B., Drits, V.A., Silvester, E., and Manceau, A. (2000) Structure of H-exchanged hexagonal birnessite and its mechanism of formation from Na-rich monoclinic buserite at low pH. American Mineralogist, 85, 826–838.

Lanson, B., Drits, V.A., Feng, Q., and Manceau, A. (2002a) Structure of synthetic

Na-birnessite: Evidence for a triclinic one-layer cell. American Mineralogist, 87, 1662–1671.
Lanson, B., Drits, V.A., Gaillot, A., Silvester, E., Plançon, A., and Manceau, A. (2002b) Structure of the heavy-metal sorbed birnessite: Part 1. Results from X-ray diffraction. American Mineralogist, 87, 1631–1645.
Libowitzky, E. (1999) Correlation of O-H stretching frequencies and O-H···O hydrogen bond lengths in minerals. Monatshefte für Chemie, 130, 1047–1059.
Libowitzky, E. and Rossman, G.R. (1997) An IR absorption calibration for water in minerals. American Mineralogist, 82, 1111–1115.
Lutz, H.D. (1988) Bonding and structure of water molecules in solid hydrates. Correlation of spectroscopic and structural data. Structure and Bonding, 69, 97–125.
McKenzie, R.M. (1971) The synthesis of birnessite, cryptomelane, and some other oxides and hydroxides of manganese. Mineralogical Magazine, 38, 493–502.
——— (1976) The manganese oxides in soils. In I.M. Varentsov and G. Grasselly, Eds., Proceedings of the 2nd International Symposium on Geology and Geochemistry of Manganese, 1, p. 259–269. Schweizerbart, Stuttgart.
——— (1977) Manganese oxides and hydroxides. In J.B. Dixon and S.B. Weed, Eds., Minerals in Soil Environments, p. 181–193. Soil Science Society of America, Madison, Wisconsin.
Moore, P.B., Araki, T., and Ghose, S. (1982) Hyalotekite, a complex lead borosilicate: its crystal structure and the lone-pair effect of Pb(II). American Mineralogist, 67, 1012–1020.
Moore, P.B., Sen Gupta, P.K., and Schlemper, E.O. (1985) Solid solution in plumbous potassium oxysilicate affected by interaction of a lone pair with bond pairs. Nature, 318, 548–550.
Nakamoto, K., Margoshes, M., and Rundle, R.E. (1955) Stretching frequencies as a function of distances in hydrogen bonds. Journal of the American Chemical Society, 77, 6480–6486.
Paterson, M.S. (1982) The determination of hydroxyl by infrared absorption in quartz, silicate glasses and similar materials. Bulletin de Minéralogie, 105, 20–29.
Post, J.E. (1999) Manganese oxide minerals: Crystal structures and economic and environmental significance. Proceedings of the National Academy of Sciences, 96, 3447–3454.
Post, J.E. and Appleman, D.E. (1988) Chalcophanite, $ZnMn_3O_7 \cdot 3H_2O$: New crystal-structure determinations. American Mineralogist, 73, 1401–1404.
Post, J.E. and Veblen, D.R. (1990) Crystal structure determinations of synthetic sodium, magnesium, and potassium birnessite using TEM and the Rietveld method. American Mineralogist, 75, 477–489.
Post, J.E., Heaney, P.J., and Hanson, J. (2002) Rietveld refinement of a triclinic structure for synthetic Na-birnessite using synchrotron powder diffraction data. Powder Diffraction, 17, 218–221.
——— (2004) In situ synchrotron X-ray diffraction study of the dehydration behaviors of Na- and K-birnessites. Geochimica et Cosmochimica Acta, 68(11s), A64.
Potter, R.M. and Rossman, G.R. (1979a) Mineralogy of manganese dendrites and coatings. American Mineralogist, 64, 1219–1226.
——— (1979b) The tetravalent manganese oxides: identification, hydration, and structural relationships by infrared spectroscopy. American Mineralogist, 64, 1199–1218.
Shannon, R.D. (1976) Revised effective ionic radii and systematic studies of interatomic distances in halides and chalcogenides. Acta Crystallographica, A32, 751–767.
Stolper, E. (1982) Water in silicate glasses: an infrared spectroscopic study. Contributions to Mineralogy and Petrology, 81, 1–17.
Taylor, R.M., McKenzie, R.M., and Norrish, K. (1964) The mineralogy and chemistry of manganese in some Australian soils. Australian Journal of Soil Research, 2, 235–248.
Wadsley, A.D. (1950) A hydrous manganese oxide with exchange properties. Journal of the American Chemical Society, 72, 1782–1784.
——— (1955) The crystal structure of chalcophanite, $ZnMn_3O_7 \cdot 3H_2O$. Acta Crystallographica, 8, 165–172.
Wilkins, R.W.T., Mateen, A., and West, G.W. (1974) The spectroscopic study of oxonium ions in minerals. American Mineralogist, 59, 811–819.

MANUSCRIPT FIRST RECEIVED FEBRUARY 11, 2005
MANUSCRIPT ACCEPTED SEPTEMBER 22, 2005
MANUSCRIPT HANDLED BY ROBERT F. DYMEK

APPENDIX 1

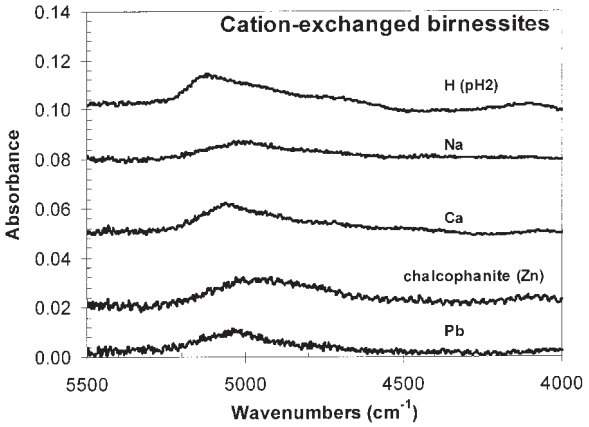

APPENDIX FIGURE 1. Near-IR spectra of H-, Na-, Ca-, and Pb-birnessites and chalcophanite. Absorption between 4800–5200 cm^{-1} is assigned to a combination mode of H_2O; the mode at ~4650 cm^{-1} in the H-birnessite spectrum is due to a combination mode of OH or H_3O^+.

[1] Deposit item AM-06-012, Appendix 2. Deposit items are available two ways: For a paper copy contact the Business Office of the Mineralogical Society of America (see inside front cover of recent issue) for price information. For an electronic copy visit the MSA web site at http://www.minsocam.org, go to the American Mineralogist Contents, find the table of contents for the specific volume/issue wanted, and then click on the deposit link there.